Preparation of nanocrystalline-coated carbon nanotube/Ni$_{0.5}$Zn$_{0.5}$Fe$_2$O$_4$ composite with excellent electromagnetic property as microwave absorber

IOP Publishing

J. Phys. D: Appl. Phys. **46** (2013) 145002 (6pp)

Journal of Physics D: Applied Physics

doi:10.1088/0022-3727/46/14/145002

Preparation of nanocrystalline-coated carbon nanotube/Ni$_{0.5}$Zn$_{0.5}$Fe$_2$O$_4$ composite with excellent electromagnetic property as microwave absorber

Xiao-Bing Zhou[1], Lu Shen[1], Lei Li[1], Tong-Ming Huang[2], Chun-Feng Hu[1], Wei-Ming Pan[2], Xi-Hai Jin[3], Jing Sun[3], Lian Gao[4] and Qing Huang[1]

[1] Ningbo Institute of Materials Technology and Engineering, Chinese Academy of Sciences, Ningbo, 315201, People's Republic of China
[2] Institute of High Energy Physics Chinese Academy of Sciences, Beijing, 100049, People's Republic of China
[3] Shanghai Institute of Ceramics, Chinese Academy of Sciences, Shanghai, 200050, People's Republic of China
[4] Shanghai Jiao Tong University, Shanghai, 200240, People's Republic of China

E-mail: huangqing@nimte.ac.cn

Abstract
A combined precipitation-hydrothermal method was used to fabricate carbon nanotube/Ni$_{0.5}$Zn$_{0.5}$Fe$_2$O$_4$ ferrite composite powders. The phase, microstructure and electromagnetic properties of CNT/Ni$_{0.5}$Zn$_{0.5}$Fe$_2$O$_4$ composites were investigated. After surface modification, The zeta potential value of CNTs could maintain at about -50 mV when pH is higher than 8, which affords a suitable surface environment for *in situ* coating of Ni$_{0.5}$Zn$_{0.5}$Fe$_2$O$_4$ nanocrystallines. With increasing CNTs content, the saturation magnetization of the composites is gradually reduced, while the complex magnetic permeability changes little. The complex dielectric constant of the composites is significantly increased when the concentration of CNTs approaches the percolation threshold value of 2 wt%. When CNTs content is 5 wt%, the reflection ratios are less than -10 dB within the frequency range 2–9 GHz, and the reflection ratios reach a minimum -32.5 dB at a frequency of about 3.9 GHz.

(Some figures may appear in colour only in the online journal)

Ni$_{0.5}$Zn$_{0.5}$Fe$_2$O$_4$ ferrite is a relatively mature electromagnetic wave absorber exhibiting good microwave absorbing performance [1, 2]; however, the poor temperature stability and high density limit its application as radar absorbing materials in stealth aircraft and other areas [3]. Carbon nanotubes (CNTs), with lager surface area, large number of dangling bonds which can cause interfacial polarization and macroscopic quantum tunnel effect, have revealed good microwave absorbing performance [4]. In addition, the light weight, good heat, corrosion and thermal shock resistance, higher thermal and electrical conductivity of CNTs have made them a promising candidate for advanced composite in recent years [5–7].

Akhtar *et al* [8] prepared Ni$_{0.8}$Zn$_{0.2}$Fe$_2$O$_4$–MWCNTs composites using the sol–gel method, and an initial permeability and the Q values of 20.043 and 50.047 of the 750 °C sintered Ni$_{0.8}$Zn$_{0.2}$Fe$_2$O$_4$–MWCNTs composite were found. Ali Ghasemi [9] found that the introduction of CNTs could significantly improve reflection loss of strontium ferrite–CNTs composite films at the 8–12 GHz band. When MWCNTs content reached 4 vol%, the reflection loss of the composites is -29 dB at a frequency of 9.7 GHz. Liu *et al* [10] prepared the CNTs–NiFe$_2$O$_4$ composites by *in situ* precipitation of metal hydroxides in ethanol on CNTs and followed by hydrothermal processing. The results showed

that the electrical conductivity is increased by 5 orders of magnitude with 10 wt% addition of surface treated CNTs. Cao *et al* [11] prepared CNTs–Ni$_{0.5}$Zn$_{0.5}$Fe$_2$O$_4$ composites by the hydrothermal method, the coercive force and saturation magnetization of which were 386 Oe and 28.82 emu g^{-1} at room temperature. Jiang *et al* [12] synthesized CNT–Fe$_3$O$_4$ composites by the *in situ* solvothermal method and found that the addition of CNTs could increase the electrical conductivity by about 32%.

In this study, we successfully fabricated CNTs–Ni$_{0.5}$Zn$_{0.5}$Fe$_2$O$_4$ composites by *in situ* coating of NiZnFe nanoparticles on the covalent bond and non-covalent bond co-modified CNTs using a coprecipitation-hydrothermal processing, based on our previous thermodynamic analysis [13, 14]. The impact of microstructure and content of CNTs on the magnetic properties and microwave absorbing properties were studied.

1. Experiment

1.1. Functionalization of CNTs

Multiwall carbon nanotubes (MWCNTs) from Shenzhen Nanotech Co., with a diameter of 40–60 nm, length of 2–10 μm and purity of more than 97% according to the supplier, were used as raw material. Covalent bond modification of CNTs was achieved by adding 1 g CNTs to 250 ml of concentrated nitric acid, refluxing at 150 °C for 5 h. Further adding 0.1 g of sodium lignin sulfonate into the filtered and re-dispersed CNTs were used to achieve non-covalent bond modification, followed by another ultrasonic dispersing process for 45 min. Finally, a covalent and non-covalent bond co-modified 1 mg ml^{-1} CNTs dispersion was obtained by repeatedly washing, filtering and re-dispersing with deionized water.

1.2. CNTs-Ni$_{0.5}$Zn$_{0.5}$Fe$_2$O$_4$ nanopowders prepared

Desired amount of 1 mg ml^{-1} CNTs dispersion was added to the salt solution composed of Ni(NO$_3$)$_2$, Zn(NO$_3$)$_2$ and Fe(NO$_3$)$_3$, in molar ratio of Ni : Zn : Fe = 0.5 : 0.5 : 2 according to stoichiometric ratio of Ni$_{0.5}$Zn$_{0.5}$Fe$_2$O$_4$, followed by magnetic stirring and ultrasonic dispersing for 30 min. According to the thermodynamic calculation in the literature [14], the pH value should be controlled at 10.5 ± 0.1 to fabricate the expected ferrite. The mixed solution of the salt and CNTs was added dropwise to 1 mol l^{-1} NaOH solution at a flow rate of 10 ml min^{-1}. After co-precipitation, Ni, Zn and Fe hydroxide precursor slurry formed and then the slurry was transferred into a PTFE vessel sealed in a stainless-steel sleeve. The hydrothermal reaction was performed at 200 °C for 3 h. After washing, drying, grinding and passing through a 200 mesh sieve, the final CNTs–Ni$_{0.5}$Zn$_{0.5}$Fe$_2$O$_4$ powder was obtained.

1.3. Characterization

X-ray diffraction (XRD, D8, Bruker, Germany) was used to analyse the sample phase. Microstructure of the composites was observed using transmission electron microscope (TEM,
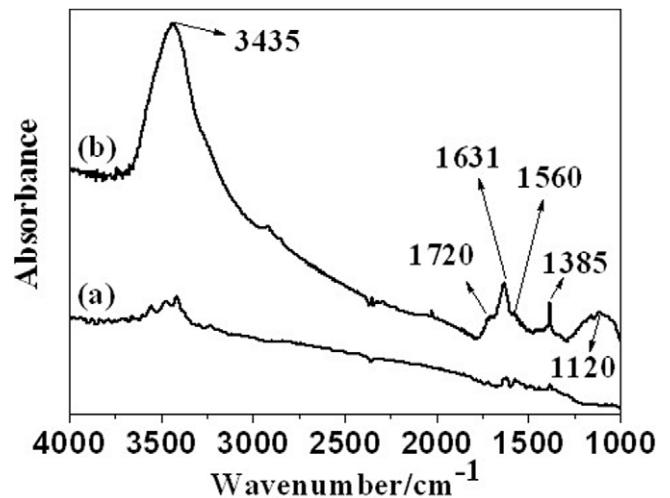

Figure 1. FTIR spectra of CNTs.

Tecnai F20, Phillip, Holland). Fourier transform infrared spectroscopy (FTIR, Thermo, Nicolet 6700, USA) was used to characterize functional groups on the surface before and after functionalization of CNTs. Electromagnetic property was measured in Physical Properties Measurement Studio (PPMS, Quantum Design, USA) at room temperature hysteresis loop. Permeability and permittivity were tested with microwave vector network analyser (8722ES, Agilent, USA).

2. Results and discussion

Figure 1 shows the FTIR spectrum of CNTs with and without functionalization. Since the surface layer of CNTs contains a small amount of adsorbed water, the original CNTs show a typical OH stretching peak of adsorbed water. Table 1 lists the characteristic absorption peak of CNTs after treatment by concentrated nitric acid and lignin sulfonate modification [10, 15]. The strong absorption peak at 3435 cm^{-1} is due to O–H stretching vibration and the 1720 cm^{-1} one corresponds to the carboxyl peak, which is formed by decomposition of the free oxygen and the carbon atom to form a carbonyl group (1631 cm^{-1}) and then the carbonyl group further reacts with H$^+$, OH$^-$ or free oxygen in water to form –COOH, during the refluxing process at 150 °C. The relatively sharp absorption peak at 1385 cm^{-1} is characterized by N=O stretching. Peak at about 1120 cm^{-1} corresponds to the C–O stretching vibration derived from lignin sulfonate prime. Lignin sulfonate is an amphiphilic polymer surfactant, with both sulfonic acid hydrophilic group, and carbon chain, phenolic hydroxyl hydrophobic group. Under the effect of van der Waals forces, hydrophobic group intertwines with CNTs self-assembly and the hydrophilic group stretches in the aqueous solution [16], which facilitates the dispersion of CNTs in water and *in situ* coating of nickel-zinc ferrite.

Figure 2 shows the Zeta potential value of CNTs after the functionalization. The Zeta potential values in the whole pH range that are tuned by diluted nitric acid and sodium hydroxide are negative. In the pH range 3–8, the Zeta potential value decreases significantly and becomes stable at

Table 1. Assignment of peaks in the IR spectrum of surface oxidized carbon nanotubes [10, 15].

Vibrational band (cm^{-1})	Assignment
3435	OH stretching [10, 15]
1720	–COOH stretching [15]
1631	H-bonded (C=O stretching) [10]
1560	–C=C stretching [10]
1385	–N=O stretching [17]
1120	C–C–O ring stretching, C–C–C asymmetric stretching [10]
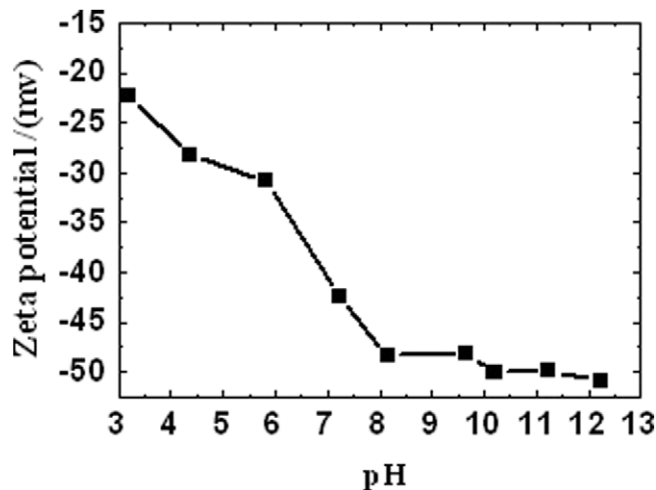
Figure 2. Zeta potential as a function of pH for surface oxidized CNTs.

about -50 mV, between pH $= 8$–12, which is slightly higher than that of Liu *et al* [16] using only sodium lignosulfonate to modify CNTs. The combination of covalent and non-covalent bond modification of CNTs can also be effective in grafting a large number of negative charges on its surface. By Coulomb repulsion between the CNTs surface, intertwining and aggregation of CNTs can be prevented.

The XRD patterns of pure $Ni_{0.5}Zn_{0.5}Fe_2O_4$ and 1 wt% CNTs–$Ni_{0.5}Zn_{0.5}Fe_2O_4$ powders before and after the hydrothermal reaction are shown in figure 3, respectively. Before hydrothermal reaction (figures 3(a) and (b)), the precursor is amorphous while after 200 °C hydrothermal reaction for 3 h, the precursor completely converted to the $Ni_{0.5}Zn_{0.5}Fe_2O_4$ spinel phase. The broadening of the diffraction peaks is caused by grain refinement, which is in accordance with figure 4(*b*). In addition, the introduction of the CNT did not change the $Ni_{0.5}Zn_{0.5}Fe_2O_4$ spinel phase.

Figure 4(*a*) is the TEM photograph of 1 wt% CNTs–$Ni_{0.5}Zn_{0.5}Fe_2O_4$, from which spherical $Ni_{0.5}Zn_{0.5}Fe_2O_4$ powders with a particle size of approximately 30 nm can be seen, coated on CNTs under the driving force of surface charge electrostatic attraction [18]. As described above, the modified CNTs have negatively charged surfaces (the Zeta potential of approximately -50 mV at pH of about 10.5), which can attract positive charged Ni^{2+}, Zn^{2+} and Fe^{3+} hydroxide in the co-precipitation and hydrothermal reaction. After 200 °C hydrothermal reaction for 3 h, spinel phase NiZn ferrite gradually crystallized on the surface of CNTs. In figure 4(*b*), selected area electron diffraction (SAED) also shows the good crystallization of NiZn ferrite coated on CNTs.
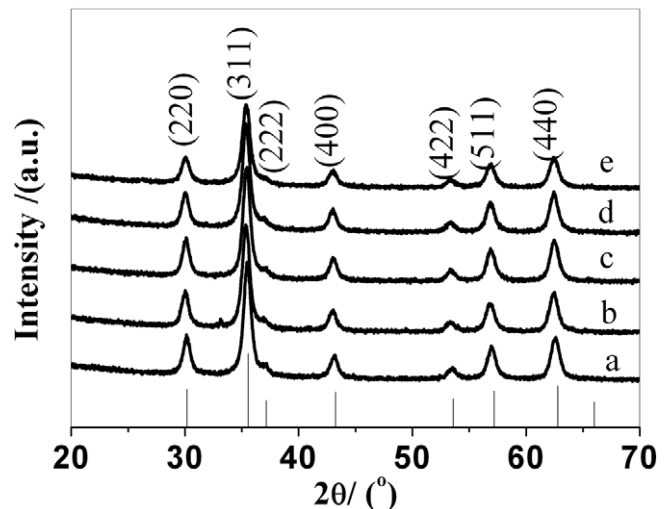

Figure 3. X-ray diffraction (XRD) patterns of precursors: (a) $Ni_{0.5}Zn_{0.5}Fe_2O_4$, (b) 1 wt% CNTs-$Ni_{0.5}Zn_{0.5}Fe_2O_4$, and precursors hydrothermally treated at 200 °C for 3h: (c) $Ni_{0.5}Zn_{0.5}Fe_2O_4$, (d) 1 wt% CNTs-$Ni_{0.5}Zn_{0.5}Fe_2O_4$.

Figure 5 is the hysteresis loop of CNTs–$Ni_{0.5}Zn_{0.5}Fe_2O_4$ powders, all exhibiting typical soft ferrite properties. The coercive force and the residual magnetization of all the composite powders are nearly zero. With the increase of CNTs, saturation magnetization of the powders gradually reduced, which is in accordance with what reported in the literature [11, 19]. Pure $Ni_{0.5}Zn_{0.5}Fe_2O_4$ nanopowders have a saturation magnetization of 61.59 emu g^{-1}, and decreased to 55.62 emu g^{-1} when added 5 wt% CNTs.

Figure 6 shows the complex magnetic permeability of composite fabricated by CNTs–$Ni_{0.5}Zn_{0.5}Fe_2O_4$ powders with paraffin (20 wt%). In the range 1–3 GHz, the real part of permeability of all the composites decreased rapidly with increasing frequency, while stabilized at 3–12 GHz with an unconspicuous wide resonance absorption peak at 5–12 GHz. The imaginary part of the magnetic permeability decreased monotonically with increasing frequency. Moreover, when the amount of CNTs is less than 2 wt%, the introduction of the CNTs has little effect on the magnetic permeability of the ferrite-based material; when CNTs content reached 5 wt%, both real and imaginary parts of permeability decreased obviously in the range 1–6 GHz, while they remained similar to other samples in the 6–12 GHz region.

Figure 7 shows the complex magnetic permeability of CNTs–$Ni_{0.5}Zn_{0.5}Fe_2O_4$ powders with different CNTs content. It can be seen that the change in dielectric constant can be divided into two categories: CNTs content lower than 1 wt% and CNTs content higher than 2 wt%. When CNTs content is lower than 1 wt%, both the real part and imaginary part of permittivity are decided by $Ni_{0.5}Zn_{0.5}Fe_2O_4$ base material, with real part varying between 7 and 9 and imaginary part varying between 0 and 1. When CNTs content is higher than 2 wt% (threshold value), the real part of the dielectric constant increased rapidly to about 15–17 and the imaginary part increased to about 3.

Chojnacki *et al* [20] and Ahmad *et al* [21] found a similar phenomenon in the CNT/alumina ceramic composite
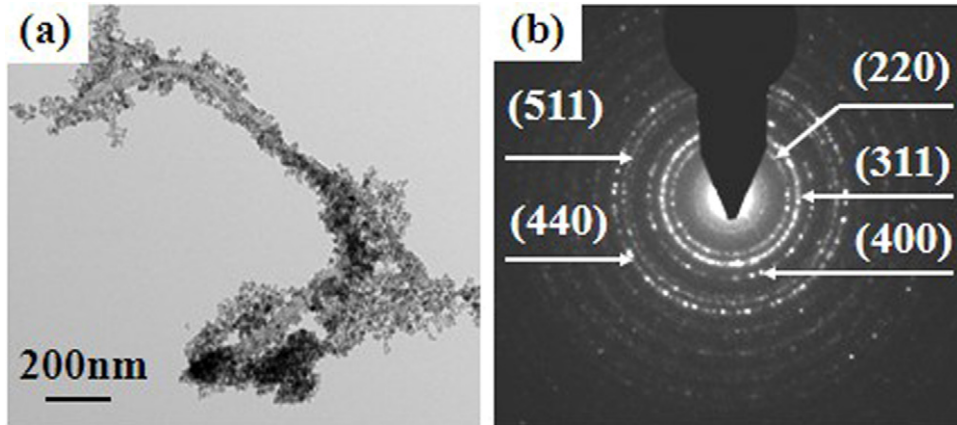
Figure 4. (*a*) TEM micrographs of 1 wt%CNTs-Ni$_{0.5}$Zn$_{0.5}$Fe$_2$O$_4$ composite powders; (*b*) SAED image of CNTs coated with Ni$_{0.5}$Zn$_{0.5}$Fe$_2$O$_4$.

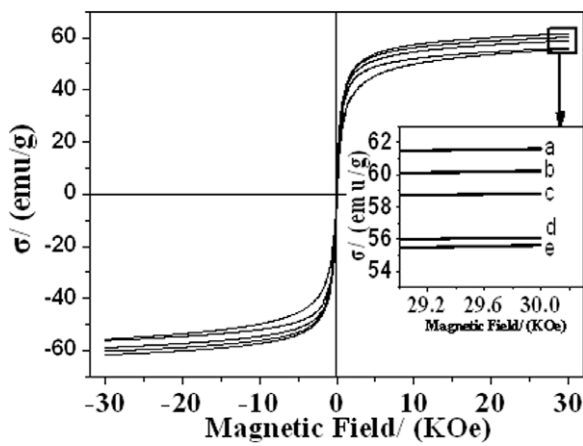**Figure 5.** Hysteresis loops of CNTs-Ni$_{0.5}$Zn$_{0.5}$Fe$_2$O$_4$ composite powders with different CNTs contents: (a) 0 wt%, (b) 0.5 wt%, (c) 1 wt%, (d) 2 wt% and (e) 5 wt%.
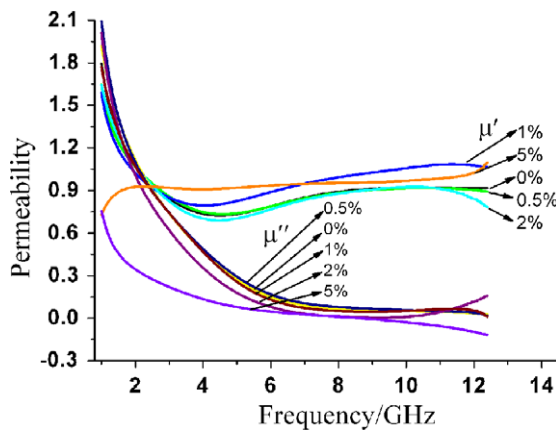

Figure 7. Complex permittivity of CNTs-Ni$_{0.5}$Zn$_{0.5}$Fe$_2$O$_4$ composites.

Figure 6. Complex permeability of CNTs-Ni$_{0.5}$Zn$_{0.5}$Fe$_2$O$_4$ composites.

system. Song *et al* [22] thought this is because the conductive network formed by CNTs in composite can be seen as small parallel plate capacitors, the polarization effects between which improves the charge storage capacity and therefore the real part of permittivity of composite. As to the increase in the imaginary part of the permittivity, Zhao *et al* [23] thought that
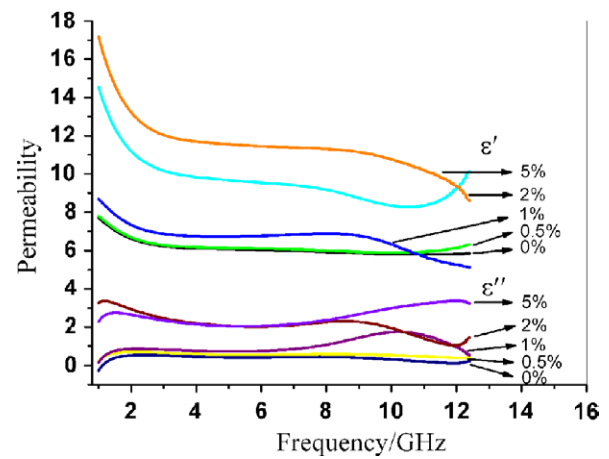
this is because of the large specific surface area, a large number of π electrons of CNTs, and the large number of interface and voids formed between CNTs and ferrite nanoparticles. Such a structure and defects in the microwave electromagnetic field make it easy to form a space charge polarization, and thereby produce a strong dielectric loss.

Utilizing excellent electromagnetic loss performance of CNTs–Ni$_{0.5}$Zn$_{0.5}$Fe$_2$O$_4$ composites, wave absorbing materials that meet the needs of various bands can be designed. Based on transmission line theory, the input impedance Z_{in} of absorbing materials at the input interface is [24]

$$Z_{in} = \sqrt{\frac{\mu_r}{\varepsilon_r}} \tanh \left[j \frac{2\pi f d}{c} \sqrt{\mu_r \varepsilon_r} \right],$$

where μ_r and ε_r are the complex magnetic permeability and the complex permittivity, respectively, f is the frequency, d is the thickness and c is the speed of light.

The reflection coefficient Γ depends on input impedance Z_{in}:
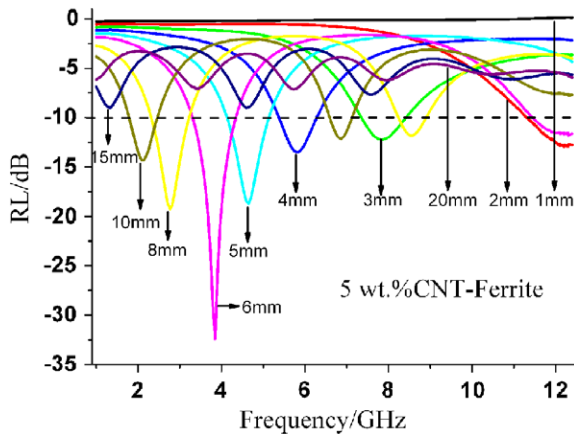
$$\Gamma = \frac{Z_{in} - 1}{Z_{in} + 1}.$$

Figure 8. Frequency dependence of the dielectric loss factor and the magnetic loss factor of 5 wt%CNTs-$Ni_{0.5}Zn_{0.5}Fe_2O_4$ dispersed in paraffin.
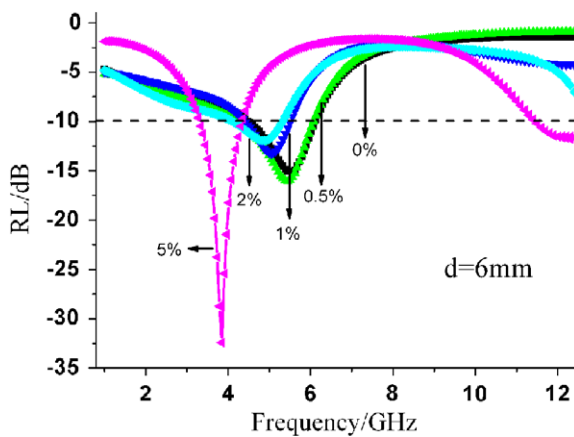

Figure 9. Frequency dependence of the dielectric loss factor and the magnetic loss factor of CNTs-$Ni_{0.5}Zn_{0.5}Fe_2O_4$ composites with different CNTs content dispersed in paraffin.

Reflectivity of absorbing materials is

$$R = 20 \log \left| \frac{Z_{in} - 1}{Z_{in} + 1} \right|.$$

It can be seen from the formulae that, for single-layer absorbing materials, the ability of microwave absorbing is decided by complex permeability, complex permittivity, the sample thickness d and the frequency used. The reflectance of 5 wt% CNTs–$Ni_{0.5}Zn_{0.5}Fe_2O_4$ and paraffin (20 wt%) composite sample at different thicknesses versus frequency was calculated with the Mathcad program (figure 8). At a thickness of 6 mm, the influence of CNTs content on absorbing performance of the CNTs–$Ni_{0.5}Zn_{0.5}Fe_2O_4$ composites was shown in figure 9.

As can be seen, for the 5 wt% CNTs–$Ni_{0.5}Zn_{0.5}Fe_2O_4$ sample, by adjusting its thickness the reflection rate can be adjusted to less than −10 dB in the range 2–9 GHz. When the designed thickness is 6 mm, with increasing nanotube content, the variation of reflectivity in CNTs–$Ni_{0.5}Zn_{0.5}Fe_2O_4$ samples is not obvious. When CNTs content is less than 0.5 wt%, the absorption peak remains constant while the reflection rate reduces from −15 to −20 dB. When

0.5 wt% ⩽ CNTs ⩽ 2 wt%, the absorption peak is moving towards the low band, and the reflectance increases to about −12 dB. When CNTs content further increases to 5 wt%, the absorption peaks continue moving towards the low frequency, and the reflectance at around 3.9 GHz appears a minimum of −32.5 dB. This indicates that the CNT/nickel-zinc ferrite composites have better application prospects as microwave absorbing material.

3. Conclusion

(1) With a combination of the covalent and non-covalent bond modification method, high density hydrophilic groups were grafted on the CNT surface to obtain a high concentration stable CNTs suspension.

(2) Based on the early thermodynamic analysis of chemical co-precipitation of nickel-zinc ferrite, further co-precipitation hydrothermal method was used to prepare nickel-zinc ferrite *in situ* coated CNT composites. The grain size of the nickel-zinc ferrite was about 30 nm and its phase was spinel-type polycrystalline structure.

(3) Then the saturation magnetization of the CNTs–$Ni_{0.5}Zn_{0.5}Fe_2O_4$ composite gradually decreased with increasing CNTs content. The pure $Ni_{0.5}Zn_{0.5}Fe_2O_4$ nanopowders had a saturation magnetization of 61.59 emu g^{-1}, while when the CNT content reached 2 wt%, the saturation magnetization is 55.62 emu g^{-1}.

(4) A threshold existed in the content of CNTs on the electromagnetic property of CNT–$Ni_{0.5}Zn_{0.5}Fe_2O_4$ composite. When the content of CNTs exceeded the threshold, electromagnetic performance of the composite changed significantly. When the content of CNTs is 5 wt%, by adjusting the thickness of the composite, absorbing materials satisfying different frequency bands can be designed. When the thickness is 6 mm, the reflectance at the 3.9 GHz is about −32.5 dB.

References

[1] Verma A and Dube D C 2005 *J. Am. Ceram. Soc.* **88** 519–23
[2] Cho S, Kang D and Oh J 1996 *J. Mater. Sci.* **31** 4719–22
[3] Chen X G, Ye Y and Cheng J P 2011 *J. Inorg. Mater.* **26** 449–57
[4] Thomassin J M *et al* 2010 *Polymer* **51** 115–21
[5] Baughman R H, Zakhidov A A and de Heer W A 2002 *Science* **297** 787–92

J. Phys. D: Appl. Phys. **46** (2013) 145002

X-B Zhou *et al*

[6] Iijima S 1991 *Nature* **354** 56–8
[7] Wu J and Kong L 2004 *Appl. Phys. Lett.* **84** 4956–8
[8] Akhtar M N *et al* 2011 *Ceram. Int.* **37** 3237–45
[9] Ghasemi A 2011 *J. Magn. Magn. Mater.* **323** 3133–7
[10] Liu Y Q and Gao L 2005 *Carbon* **43** 47–52
[11] Cao H *et al* 2007 *J. Solid State Chem.* **180** 3218–23
[12] Jiang L and Gao L 2003 *Chem. Mater.* **15** 2848–53
[13] Zhou X B *et al* 2009 *Chin. J. Inorg. Chem.* **25** 602–8
[14] Zhou X B, Dai J Q and Cai J H 2009 *J. Chin. Ceram. Soc.* **37** 23–8
[15] Kim S D *et al* 2007 *J. Fluorine Chem.* **128** 60–4
[16] Liu Y, Gao L and Sun J 2007 *J. Phys. Chem.* C **111** 1223–9
[17] Konstantin I H 2000 *Catal. Rev.* **42** 71–144
[18] Sun J and Gao L 2006 *J. Electroceram.* **17** 91–4
[19] Zhang Y *et al* 2010 *J. Magn. Magn. Mater.* **322** 2006–9
[20] Chojnacki E *et al* 2011 *Nucl. Instrum. Methods Phys. Res.* A **659** 49–54
[21] Ahmad K, Pan W and Shi S L 2006 *Appl. Phys. Lett.* **89** 133122
[22] Song Y *et al* 1986 *Phys. Rev.* B **33** 904
[23] Zhao D L and Shen Z M 2005 *J. Inorg. Mater.* **20** 608–12
[24] Mu G *et al* 2008 *Mater. Lett.* **62** 840–2